Published in final edited form as:

Mol Cancer Res. 2018 August ; 16(8): 1319–1331. doi:10.1158/1541-7786.MCR-17-0589.

Novel Regulation of Integrin Trafficking by Rab11-FIP5 in Aggressive Prostate Cancer

Lipsa Das[1], **Jaime M.C. Gard**[5], **Rytis Prekeris**[6], **Raymond B. Nagle**[3,5], **Colm Morrissey**[7], **Beatrice S. Knudsen**[8], **Cindy K. Miranti**[2], and **Anne E. Cress**[2,4,5,*]

[1]Cancer Biology Graduate Interdisciplinary Program, University of Arizona, Tucson, AZ 85724

[2]Cellular and Molecular Medicine, University of Arizona, Tucson, AZ 85724

[3]Pathology, University of Arizona, Tucson, AZ 85724

[4]Molecular and Cellular Biology, University of Arizona, Tucson, AZ 85724

[5]The University of Arizona Cancer Center, University of Arizona, Tucson, AZ 85724

[6]University of Colorado, Anschutz Medical Campus, Aurora, CO 80045

[7]University of Washington, Seattle, WA 98195

[8]Cedars Sinai Medical Center, Los Angeles, CA 90048.

Abstract

The laminin-binding integrins, α3β1 and α6β1, are needed for tumor metastasis and their surface expression is regulated by endocytic recycling. β1 integrins share the Rab11 recycling machinery but the trafficking of α3β1 and α6β1 are distinct by an unknown mechanism. Using a mouse PDX tumor model containing human metastatic prostate cancer, Rab11 family interacting protein 5 (Rab11-FIP5) was identified as a lead candidate for α6β1 trafficking. Rab11-FIP5 and its membrane binding domain were required for α6β1 recycling, without affecting the other laminin-binding integrin (i.e., α3β1) or unrelated membrane receptors like CD44, transferrin receptor, or E-cadherin. Depletion of Rab11-FIP5 resulted in the intracellular accumulation of α6β1 in the Rab11 recycling compartment, loss of cell migration on laminin, and an unexpected loss of α6β1 recycling in cell-cell locations. Taken together, these data demonstrate that α6β1 is distinct from α3β1 via Rab11-FIP5 recycling and recycles in an unexpected cell-cell location.

Keywords

integrin; laminin; recycling kinetics; endosomes; Rab11; prostate cancer

[*]Corresponding Author Anne E. Cress, Department of Cellular and Molecular Medicine, The University of Arizona Cancer Center, 1515 N. Campbell Ave., Tucson, AZ 85724, USA, Tel.: (520) 626-7553, Fax: (520) 626-4979, cress@email.arizona.edu.

The authors declare no potential conflicts of interest.

INTRODUCTION

Integrins are evolutionarily conserved heterodimeric transmembrane receptors expressed on the cell surface that interact with the surrounding extracellular matrix to regulate cell adhesion, migration and signal transduction between internal and external cellular environments (1). The laminin-binding integrins (heterodimers containing α3 and α6 subunits α3β1, α6β1, and α6β4) are essential in various stages of development and maintenance of adult tissue (2, 3). In normal adult polarized tissue, they are restricted to the basolateral localization (4). However, dynamic changes in the membrane expression and localization of these integrins is observed during various normal cell processes associated with active cellular migration, such as epithelia formation during development (5), rostral migratory stream migration during brain development (6), or wound healing (7, 8). Similarly, in invasive cancer this phenomenon is amplified (9).

Intracellular trafficking of integrins is an important determinant of membrane expression and localization of integrins, and hence their function. Membrane integrins are continuously internalized, sorted through intracellular vesicular compartments and returned back to the cell surface by recycling (10). The rate of recycling determines the flux of integrins on the membrane and is key to cell migration (11). Once internalized, membrane receptors travel through a cascade of intracellular vesicular compartments defined by a family of small GTPases called Rab GTPases (12, 13). Rab11 is one such major trafficking regulator that marks the perinuclear recycling compartment (PNRC; also called apical recycling endosomes, ARE) and is a central hub of cellular trafficking to transport a variety of proteins from intracellular compartments to the plasma membrane (14). The role of Rab11 in trafficking of integrins is well known (15) its deregulation being a key feature of cancer (16, 17). Integrin α6β4 is known to be recycled by Rab11 in both normal and cancer cells. In breast cancer, Rab11 mediated α6β4 recycling is associated with hypoxia induced cancer invasion (17). Rab11 dependent α6 integrin recycling is important for rapid motility of cranial neural crest cells on laminin (18).

Despite sharing the same beta partners or extracellular ligands, integrins follow distinct temporal and spatial trafficking routes, selectivity determined by the alpha subunit (15, 19). Most integrins including the laminin-binding integrins, share the central Rab11 recycling machinery and additional regulators are likely involved in providing selectivity to different integrins. A group of Rab11 effector proteins called Rab11 family interacting proteins (Rab11-FIPs) are important candidates for recruiting specific proteins to Rab11 as they regulate various temporally and spatially distinct steps of Rab11 dependent recycling (20, 21). Rab11-FIPs are known to recycle a selective, although not necessarily exclusive, repertoire of cargo, including integrins (20). For example, α5β1 integrin is trafficked by Rab11-FIP1 but no other class I Rab11-FIPs (Rab11-FIP2 or Rab11-FIP5) (11), suggesting Rab11-FIPs can provide specificity to recycling of specific integrins based on different alpha subunits. Rab11-FIPs localize to discrete subdomains in Rab11 recycling endosomal tubules (21) through a conserved C-terminal Rab11 binding domain (RBD) (22, 23). Class I Rab11-FIPs (Rab11-FIP1, Rab11-FIP2, Rab11-FIP5) contain the C2 domain that binds to membrane phosphoinositides required for docking to membrane (24). Class II Rab11-FIPs (Rab11-FIP3, Rab11-FIP4) instead contain a calcium binding EF hand motif and are crucial

in intracellular transport during cell division, especially formation of the cleavage furrow. Rab11-FIPs also provide directionality in vesicular movement and can be involved in both anterograde trafficking from early endosomes to a Rab11 compartment as well as from a Rab11 compartment to the plasma membrane (25).

Here we report Rab11-FIP5 as a recycling regulator specific to α6 integrin that does not affect other integrins trafficked by Rab11, including the other laminin-binding α3 integrin. In effect, we offer a solution to the problem of how α3 and α6 integrins have different trafficking kinetics despite having the same β1 integrin subunit partner. Depletion of Rab11-FIP5 significantly reduced recycling of α6 integrin, a known pro-migratory integrin (26, 27) and inhibited cell migration, adding a new way to interrupt α6 integrin function.

MATERIALS AND METHODS

Cells and Reagents:

Human prostate cancer cell line DU145 from brain metastasis (American Type Culture Collection (ATCC), Manassas, VA) and PC3N cell line, an N-cadherin expressing variant of bone metastatic human prostate carcinoma cells PC3 (28), were grown in Iscove's modified Dulbecco's medium (IMDM) (Invitrogen, Carlsbad, CA) supplemented with 10% fetal bovine serum (FBS), Hyclone Laboratories (Novato, CA), at 37 °C in a 5% CO_2 humidified incubator. Trypsin-EDTA (Gibco, NY) or non-enzymatic Cellstripper (CellGro, Manassas, VA) were used to disassociate adherent cells. HaCaT were grown in Dulbecco's medium (Invitrogen) and laminin-511 and laminin-332 enriched conditioned media was harvested. All cell lines are used within 15 passages of thawing and use in the experiments and authenticated using the University of Arizona Genetics Core service that uses autosomal STR profiles for verification using reference database at ATCC. Mycoplasma testing is routinely performed on a semi-annual basis by the University of Arizona Cancer Center Core services.

The GFP tagged mutant Rab11-FIP5 constructs characterized earlier (29) were a kind gift from Dr. Rytis Prekeris (University of Colorado, Denver, CO). They were transfected into PC3N cell line using lipofectamine 2000 (Invitrogen) as per manufacturer's protocol and stable clones were selected using G418 and sorted using the FACSAria III (BD Biosciences, San Jose, CA).

2% formaldehyde was used to fix cells, 0.2% Triton X-100 in PBS for permeabilization and PBS was used for all washes in flow cytometry and immunofluorescence protocols.

Antibodies (listed based on experiments):

Membrane expression analysis by flow cytometry − anti-α6 integrin rat phycoerythrin (PE) conjugated GoH3 (eBiosciences, San Diego, CA), anti-β4 integrin eFluor 660 conjugated 439–9B (eBiosciences), anti-α3 integrin rabbit AB1920 (Chemicon, Temecula, CA), mouse CD44 antibody (Cell Signaling Technologies, CST, Danvers, MA), rabbit E-cadherin (CST), anti-rabbit AlexaFluor 488 (A488), AlexaFluor 633 (A633), or anti-mouse A633 conjugated secondary antibody (Invitrogen). PE or A488 conjugated GoH3 (eBiosciences) were used in α6 integrin internalization and recycling assay, respectively. Anti-α3 integrin fluorescein-

conjugated IA3 (FAB1345, R&D Systems, Minneapolis, MN) or FITC-conjugated anti-transferrin receptor CD71 (TfR) antibody (eBiosciences) were used for both internalization and recycling assays. Anti-A488, anti-Fluorescein (Invitrogen), and anti-FITC monoclonal antibody (Abcam, Cambridge, MA) were used for fluorophore quenching in recycling assay.

Antibodies for immunofluorescence staining: anti-α6 integrin J1B5 rat monoclonal antibody, anti-EEA1 (Early Endosome Antigen-1) polyclonal rabbit antibody (CST #2411), anti-Rab11a rabbit polyclonal antibody (CST #2413), anti-rat Alexa 568, anti-rabbit Alexa 488 conjugated secondary antibodies (Invitrogen), or anti-rabbit DyLight 650 conjugated secondary antibody (BD Biosciences).

Antibodies for western blotting: anti-α6 integrin antibody AA6NT (27), anti-α3 integrin rabbit AB1920 antibody (Chemicon), anti-Rab11a (CST), anti-Rab11-FIP5 rabbit polyclonal (Novus Biologicals, Littleton, Colorado) and horseradish peroxidase–conjugated secondary antibodies (Jackson Immuno-Research Laboratories Inc., West Grove, PA). Anti-=α6 integrin antibody GoH3 was used for blocking the adhesion function of the integrin.

Flow cytometry of membrane expression:

DU145 or FIP5-GFP mutant PC3N cells obtained with Cellstripper were fixed, blocked and incubated with receptor specific antibodies for 30 minutes followed by PBS washes and 20 minutes incubation with respective secondary antibodies. Unbound secondary antibodies were washed off and fluorescence of labeled cell surface receptors was measured using BD Accuri C6 flow cytometer (BD Biosciences).

Human prostate tissue microarray and Immunohistochemistry:

Tissue microarray (TMA) specimens were obtained as part of the University of Washington Medical Center Prostate Cancer Donor Program, approved by the University of Washington Institutional Review Board (30). The patient TMA was constructed with 1 mm-diameter duplicate cores from 44 patients with castration-resistant prostate cancer (185 metastatic sites of which 121 are bone metastases and 64 are soft tissue metastases) (31). The soft tissue metastatic sites included 35 lymph nodes, 19 livers, and 10 other soft tissue sites. The LuCaP PDX TMA was constructed with 1 mm-diameter duplicate cores established from patients with castration-resistant metastatic prostate cancer (32).

Tissues were retrieved using Na/EDTA buffer pH 8.0 and immunohistochemistry performed using the AA6NT antibody (1:700) on the Discovery XT Automated Immunostainer (Ventana Medical Systems, Inc., Tucson, AZ). Membrane and cytoplasmic staining were scored by a pathologist (BSK).

Flow cytometry internalization/recycling assay:

The internalization assays were performed as previously described (33). For recycling assay, cell surface receptors were labeled with fluorophore-conjugated antibodies at 37°C in 10% FBS supplemented media for 60 minutes for maximum internalization. Fluorescence of uninternalized antibodies left on the cell surface was quenched by incubating with respective anti-fluorescent quenching antibodies at 4°C for 30 minutes. Intracellularly protected

fluorescent antibody labeled receptors were allowed to recycle back to the cell surface at 25°C and quenched same as earlier. Cells were fixed and analyzed using BD Accuri C6 flow cytometer. The amount of recycled label was measured as a loss of intracellular signal and plotted as a percent of total internalized intracellular label (mean ± standard deviation). A first-order kinetics model ($y= a+b [1-exp (-k_{obs}t)]$) was fitted ($R^2>0.98$) using KaleidaGraph (Synergy Software, Reading, PA) to obtain the recycling curve where, y is the amount of receptor recycled at time t (min), b is the total amount of receptor recycled, and k_{obs} is the observed first-order rate constant (min^{-1}) (34). Actual recycling rate constant k_{actual} ($=b*k_{obs}$) was calculated as a measure of net recycling rate at the steady state. All values are reported as mean ± standard error.

Immunofluorescence:

DU145 cells grown to 70% confluence on glass coverslips were incubated with anti-α6 integrin antibody diluted to 1:100 IMDM+10% FBS media 37°C for 40 minutes. The cells were fixed, permeabilized, blocked and incubated with primary antibodies against endocytic markers EEA1 (1:100) and Rab11a (1:100) for 30 minutes followed by PBS washing and incubation with anti-rat A568 and either anti-rabbit A488 or anti-rabbit DyLight 650 conjugated secondary antibodies for 20 minutes. The nucleus was stained by incubation with 4', 6-diamidino-2-phenylindole (DAPI) (NucBlue, Molecular Probes, Eugene, OR) for 10 minutes. Coverslips were washed with water and mounted on slides using Prolong diamond antifade (Invitrogen). Images were acquired using a DeltaVision Core system (GE Healthcare BioSciences, Pittsburgh, PA) equipped with an Olympus IX71 microscope, a 60X objective (NA 1.20), deconvolved with softWoRx v1.2 (Applied Precision, Issaquah, WA), and analyzed using ImageJ Just Another Colocalization Plugin (JACoP).

Immunofluorescence imaging-based recycling assay:

Adherent cell monolayer of DU145 cells grown on glass coverslips were reacted with anti-α6 integrin rat antibody (J1B5) or anti-α3 integrin rabbit antibody (P1B5) at RT (75 minutes and 40 minutes for α6 and α3 integrins, respectively) to allow "one cycle" surface labelling and internalization of antibody bound integrin. Uninternalized integrin at the cell surface was blocked by incubating with anti-rat or anti-rabbit A564 fluorophore conjugated antibody at 4°C for 30 minutes. Cells were then incubated at RT for 0, 10, 20 and 40 minutes (with or without 0.5 mM primaquine (Invitrogen), a recycling inhibitor) to allow recycling of internalized J1B5 or P1B5 labeled integrin. Cells were fixed and recycled integrin was stained with anti-rat or anti-rabbit A488 fluorophore conjugated antibody. Nucleus was stained with DAPI and coverslips were mounted on slides as explained earlier and imaged using the 40X objective (NA 1.20) of the DeltaVision Core system. Average pixel intensity of recycled label was measured using ImageJ and reported standardized per number of cells.

Cell migration assay:

Approximately 15,000 cells (siRNA or 1mg/ml GoH3 treated) in 200 μL IMDM were plated onto the upper chamber of cell culture inserts (BD Biosciences) of pore size 8 μm coated with laminin enriched 50 μL HaCaT conditioned and allowed to migrate towards 600 μL IMDM plus 10% FBS in a 24-well tissue culture plate for 6 hours at 37°C. Cells on the underside of the insert were fixed and stained with DAPI. The average number of cells/field-

of-view was counted in fifty sections per insert using the 20X objective and “Analyze particles” plugin of ImageJ.

Statistical analysis:

Student’s t-test for unpaired samples was used throughout. One-way analysis of variance (ANOVA) with post-hoc student’s t-test was employed in Fig. 3. For internalization/recycling assays, statistical significance is tested for each timepoint and for the calculated rate kinetic parameters using student’s t-test for unpaired samples assuming unequal variance. A P-value lower than 0.05 was considered statistically significant.

RESULTS

Intracellular expression of α6 integrin in aggressive human prostate cancer correlated with Rab11-FIP5 mRNA expression:

Human prostate cancer tissues were analyzed by immunohistochemistry to determine the cellular localization of α6 integrin. Membrane staining of α6 integrin was readily observed between tumor cells. Tumor cells that had invaded the normal nerve structures, a characteristic of aggressive prostate cancer, contained an intracellular localization of α6 integrin (Fig. 1A). Since intracellular staining in clinical tissues is observed similar to those reported with Rab11 dependent cargos in model systems (25), we next analyzed gene expression patterns in a patient derived xenograft model. Rab 11 dependent cargos can accumulate in the cytoplasm on their way to membrane specific domains, using the “long loop” recycling pathway through the perinuclear recycling compartment (PNRC). A tissue microarray of 185 metastatic sites (121 bone metastases and 64 soft tissue metastases including 35 lymph nodes, 19 livers and 10 other soft tissue sites) from 44 patients was stained for α6 integrin and revealed primarily cytoplasmic expression of α6 integrin in metastatic cancer cells. 76% of bone metastases showed positive cytoplasmic expression of the integrin and 26% revealed intense cytoplasmic staining. Similarly, 82% of soft tissue metastases were positive for cytoplasmic α6 integrin with intense staining in 38% of cases (Fig. 1B). The mRNA expression profile of patient-derived mouse xenografts (PDX) from the LuCaP series established from patients with castration-resistant metastatic prostate cancer (32) was evaluated for expression of genes encoding trafficking proteins. A LuCaP PDX tissue microarray was stained for α6 integrin and the association of genes encoding trafficking proteins with cytoplasmic α6 integrin staining was tested. Top 10 genes with significant positive (>0.24) or negative (<−0.16) Pearson’s coefficient of correlation to cytoplasmic α6 integrin are reported in Fig. 1C. Interestingly, Rab11-FIP5 was identified as the most correlated (Pearson coefficient, 0.53; Fig. 1C).

Cell membrane expression of α6 integrin requires Rab11-FIP5:

Rab11-FIP5 was tested as a candidate for regulation of cell surface expression of α6 integrin. Cell membrane levels of α6 and α3 integrins, non-integrin cell adhesion receptors CD44 and E-cadherin were measured in prostate cancer cell line DU145 using surface labelling of the receptors and flow cytometry. The flow cytometry profile for α6 integrin showed that the mean peak fluorescence (MPF) was markedly reduced after silencing of Rab11-FIP5 (siFIP5) compared to untreated and non-targeting siRNA treated cell population

(siCon) (Fig. 2A). In addition, the distribution of siFIP5 cells overlapped with α6 integrin depleted cells (si α6) (Fig. 2A). The cell surface expression of the other laminin-binding integrin, α3 integrin, the non-laminin-binding cell surface receptor CD44 and cell-cell adhesion receptor E-cadherin remained unchanged in siFIP5 or si α6 cells. The MPF of surface integrin label was significantly reduced by ~50% for α6 integrin (**$p<0.01$, n=5; Fig. 2B). The total protein expression as tested by immunoblotting of α6 and α3 integrins and Rab11 in lysates was not altered upon silencing Rab11-FIP5 (Fig. 2C).

Depletion of Rab11-FIP5 reduces cell migration:

Since Rab11-FIP5 depleted cells had significant reduction of α6 integrin membrane expression and α6 integrin is known for its pro-migratory function (18, 27), we tested if the cancer cell motility is compromised. Migration of Rab11-FIP5 depleted cells was tested using a modified Boyden chamber assay, with laminin coated underside and 10% FBS supplemented media as chemoattractant. Two different siRNAs against Rab11-FIP5 had a similar effect on the migration of DU145 cells which was reduced by 42% in siFIP5 (#1) (***$p<0.001$, n=3) and 52% in siFIP5 (#2) treated cells as compared to the untreated cells (**$p<0.01$, n=3; Fig. 2D). The migration was confirmed to be α6 integrin dependent, as blocking of integrin function by the GoH3 antibody blocked cell migration by 45% (***$p<0.001$, n=3).

The C2 domain of Rab11-FIP5 is required for the membrane expression of α6β1 integrin:

Next, we assessed the functional domain of Rab11-FIP5 that would be important for α6β1 integrin membrane expression using PC3N cells, a β4 null cell line (Supplementary Fig. 1). For this, we tested Rab11-FIP5 mutants with defects in two key functionally conserved domains – the Rab11 binding domain (RBD) and the membrane phosphoinositide binding C2 domain. We tested α6 integrin membrane expression in PC3N cell line stably transfected for either of the three mutant Rab11-FIP5 proteins fused to GFP: (i) full-length Rab11-FIP5 (FIP5-GFP), (ii) a dominant negative truncated Rab11-FIP5 protein lacking the C2 domain (ΔC2FIP5-GFP), and (iii) ΔC2FIP5-GFP with a point mutation resulting in a Rab11 binding deficient Rab11-FIP5 (I630E-C2FIP5-GFP). I630E-ΔC2FIP5-GFP cannot be recruited to the Rab11 vesicles, hence is non-functional and used as a control. The mutant proteins have previously been characterized and were shown to act as a Rab11-FIP5 dominant-negative mutant (29, 35, 36). Flow cytometry profiles show a loss of α6 integrin at the membrane upon expression of the ΔC2FIP5-GFP (Fig. 3A). The MPF of membrane α6 integrin was significantly reduced by ~25% in ΔC2FIP5-GFP as compared to untransfected, FIP5-GFP transfected, or the non-functional I630E-ΔC2FIP5-GFP transfected PC3N cells (ANOVA, *$p<0.05$, n=4) (Fig. 3B). The flow cytometry profiles of membrane α3 integrin completely overlapped in each of the mutant cell lines (Fig. 3A) and the MPF remained unchanged (Fig. 3B). These results demonstrate that the C2 domain of Rab11-FIP5 selectively regulates membrane expression of α6β1 and not of α3β1 integrin. The expression of mutant FIP5-GFP protein in respective mutant cell line is shown by immunoblotting (Fig. 3C). The endogenous Rab11-FIP5 protein expression or the total expression of either α6 or α3 integrin was unaltered in each of the mutant cell line (Fig. 3C). A schematic representation of the Rab11-FIP5 mutants used is shown (Fig. 3D).

Depletion of Rab11-FIP5 increases intracellular accumulation of α6 integrin:

Since Rab11-FIP5 affects the membrane expression of α6 integrin without affecting total cellular integrin levels, we tested if the internalization rate or total amount of integrin internalized was affected. Time courses of internalization of α6 integrin, α3 integrin and the transferrin receptor (TfR, CD71) in DU145 cells are shown (Fig. 4A). Internalization curves obtained using a first order kinetic model for α6 and α3 integrins and TfR were compared between untreated control and siFIP5 cells (Fig. 4A). The percent α6 integrin internalized was not significantly different between untreated control and siFIP5 cells for the first 5 time-points tested. However, there was a significant increase in the internalized α6 integrin in siFIP5 cells after 75 minutes (*$p<0.05$, n=5), when the internalization reaches the maximum and a steady state. There were no differences in amounts of internalized α3 integrin or TfR at any time-points in the Rab11-FIP5 depleted cells (Fig. 4A). In one cycle of internalization in untreated cells, 46% of the total labeled α6 integrin was internalized and accumulated intracellularly, while in siFIP5 cells, the amount of internalization was significantly greater reaching 58% (*$p<0.05$, n=5; Fig. 4B). The internalization rate was not altered in untreated control and siFIP5 cells for either α6 (k_{actual} 1.48 min^{-1}, 1.45 min^{-1} respectively) or α3 integrin (0.69 min^{-1}, 0.87 min^{-1}). The internalization kinetics of TfR, an unrelated transmembrane protein, were also unaltered in siFIP5 or control cells with unchanged internalization rate (9.66 min^{-1}, 10.37 min^{-1}, respectively) or intracellular accumulation (60.38%, 57.62%, respectively).

Internalized α6 integrin accumulated in early endosomes and Rab11a positive PNRC:

Next, we investigated which intracellular vesicular compartments contained the internalized α6 integrin on depletion of Rab11-FIP5 protein. To increase intracellular accumulation, live untreated control or siFIP5 DU145 cells were incubated with anti-α6 integrin antibody, J1B5, for 40 minutes. Cells were then fixed, permeabilized and stained with antibodies reactive to early endosome antigen 1 (EEA1) and Rab11a to visualize α6 integrin in early endosomes or in the PNRC, respectively. In untreated control cells, α6 integrin was observed localized both at the cell membrane, primarily in cell-cell adhesion sites, and within the cytoplasm (Fig. 5A, red). Rab11a was distributed in vesicles close to the nucleus (Fig. 5A, green), as expected (37). The overlay of both images from untreated control cells revealed that α6 integrin and Rab11a primarily colocalized at sites of cell-cell adhesion. Depletion of Rab11-FIP5 increased the abundance of intracellular α6 integrin (Fig. 5B, red) in early endosomes (Supplementary Fig. 2) and the Rab11a marked PNRC (Fig. 5B). About a 2-fold increase from 16% to 29% of α6 integrin in early endosomes occurred upon Rab11-FIP5 depletion (*$p<0.05$, n=4; Fig. 5C). The Pearson's coefficient for colocalization of α6 integrin and EEA1 also increased significantly from 0.41 for untreated cells to 0.60 for siFIP5 cells (*$p<0.05$, n=4; Fig. 5C, Supplementary Fig. 2). While 34% of the α6 integrin colocalized with Rab11a vesicles in untreated cells, depletion of Rab11-FIP5 led to a significant increase of up to 56% (**$p<0.01$, n=4; Fig. 5C). The Pearson's coefficient for colocalization increased from 0.46 for untreated to 0.62 for siFIP5 cells (*$p<0.05$, n=4). The magnified cross sections showed that while α6 integrin and Rab11a primarily colocalized at cell-cell adhesion sites in untreated control cells (white triangles, Fig. 5D), depletion of siFIP5 resulted in a shift in the location of α6 integrin to the Rab11a positive PNRC (white arrows, Fig. 5D). Taken together, the data showed that depletion of Rab11-FIP5 changed the

distribution of α6 integrin from sites of cell-cell adhesions to intracellular early endosomes and Rab11a-positive vesicles. However, Rab11-FIP5 loss did not affect trafficking of α6 integrin from early endosomes to the Rab11a compartment.

Depletion of Rab11-FIP5 reduces recycling of α6 integrin:

The reduced cell surface levels and increased intracellular accumulation of α6 integrin in Rab11+ PNRC compartment upon Rab11-FIP5 depletion suggested a possible defect in integrin recycling to the cell membrane. We measured the recycling kinetics of α3, α6 integrins and the TfR using a flow cytometry approach in DU145 cells treated with two different siRNAs against Rab11-FIP5 (siFIP5(#1) or siFIP5(#2)). The recycling assay was performed at the lower temperature of 25°C to decrease the rate of recycling and to improve the resolution of the rate kinetic curve. The amount of recycled protein was plotted as the percent of total amount of internalized receptor. The recycling curve was obtained by fitting a first order kinetic model (Fig. 6A). For all four time-points tested, the amount of α6 integrin that was recycled from the cytoplasm to the cell surface was significantly reduced in the Rab11-FIP5 depleted cells compared to untreated control cells. No differences were observed for α3 integrin or TfR (Fig. 6A).

Depletion of Rab11-FIP5 using either of the two different siRNAs led to a significant ~2-fold reduction in the rate of α6 integrin recycling from 2.06 min^{-1} to a k_{actual} of 1.22 min^{-1} for siFIP5(#1) and 1.08 min^{-1} for siFIP5(#2) (**$p<0.01$, n=5; Fig. 6B). The total amount of receptor recycled in one cycle was also significantly reduced from 36% in untreated control to 29% in siFIP5(#1) and 30% in siFIP5(#2) cells (*$p<0.05$, n=5). This was consistent with the reduced membrane expression of α6 integrin in siFIP5 cells, as seen in figure 2. As expected, similar reduction in rate of recycling for β4 integrin and consequent reduction in its cell membrane expression was observed due to reduced α6 integrin recycling (Supplementary Fig. 3). About 17% of the internalized α3 integrin is recycled in one cycle of recycling in DU145 cells at a rate of 1.33 min^{-1}, which remains unaltered in siFIP5 cells (1.21 min^{-1} for siFIP5 (#1) and 1.38 min^{-1} for siFIP5 (#2); Fig. 6B). The rate of recycling of TfR is at least 5-fold faster than that of integrins (k_{actual} 11.12 min^{-1}) and remained the same in siFIP5(#1) (k_{actual} 10.20 min^{-1}) or siFIP5(#2) (k_{actual} 10.29 min^{-1}) cells. The total amount of TfR recycled also remained unchanged (21% untreated, 20% siFIP5 (#1) and 21% siFIP5 (#2); Fig. 6B). These results confirm the key and specific role of Rab11-FIP5 in α6 integrin recycling without affecting the other laminin-binding α3 integrin or the TfR.

α6 integrin is recycled to cell-cell adhesion sites:

We next identified the locations of recycled α6 integrin using adherent monolayer of DU145 cells. In short, surface α6 integrin was immunolabeled with J1B5 followed by internalization for 75 minutes for maximum intracellular accumulation. The total labeled α6 integrin at the cell membrane and internalized are shown (Fig. 7A). The uninternalized membrane integrin bound to J1B5 was labeled with a fluorescent secondary antibody (Fig. 7B, red) and appeared in both cell-cell adhesions (closed white triangles) and lamellipodia (open white triangles). Intracellular J1B5 labeled α6 integrin was then allowed to recycle and the cell surface-associated recycled protein was stained with a secondary antibody conjugated with a different fluorophore. Interestingly, within 10 minutes, the recycled α6

integrin (Fig. 7B, green) was detected only at the cell-cell adhesion sites (indicated by white arrows) and not in the lamellipodia. There was a marked increase in recycled label by 40 minutes, primarily in cell-cell locations and not lamellipodia. The recycled label disappeared upon treatment with primaquine, a recycling inhibitor. The amount of label recycled was defined by average pixel intensity of the recycled label and plotted as a bar graph for different timepoints (Fig. 7C). Levels of recycled α6 integrin increased significantly from 0 minute (104×10^3) to 10 minutes (368×10^3), 20 minutes (689×10^3) and 40 minutes (774×10^3) (**$p<0.01$, $n=3$).

Similar experiments were performed to determine the recycling location of a laminin binding α3 integrin using α3 integrin specific P1B5 antibody. The total labeled α3 integrin after 40 minutes of maximum internalization is shown (Fig. S4). The integrin was observed on cell membrane, both at the cell-cell locations and at the lamellipodia in the cell front. After allowing 40 minutes of internalization of P1B5 labeled surface α3 integrin, the uninternalized integrin (Fig. S4B, red) was primarily found at the lamellipodia (open white triangles). Intracellular P1B5 labeled α3 integrin that was recycled back to the cell surface was stained after 10 and 40 minutes of recycling (Fig. S4B, green). Unlike α6 integrin, the intracellular α3 integrin that was recycled back to the cell surface primarily appeared at the lamellipodia at the cell front within 10 minutes. Only minor staining of the α3 integrin was observed at the cell-cell locations (Fig. S4B, close white triangles). Similar distribution of recycled α3 integrin at the lamellipodia was observed at 40 minutes which was blocked by treatment with the recycling inhibitor, primaquine (Fig. S4B bottom panel).

DISCUSSION

Intracellular trafficking and subsequent recycling of integrins is an important determinant of their cell membrane expression and distribution and hence their function. Almost all integrins are known to employ the general Rab11 recycling machinery for transfer from the cytoplasm to the plasma membrane (14). Despite this, each integrin heterodimer is known to have distinct trafficking characteristics (19, 33), suggesting that different Rab11 effectors might regulate the trafficking of individual integrins. Rab11-FIPs are possible candidates to render such specificity as they are known to recycle a selective, although not necessarily exclusive repertoire of cargo including integrins. Here, we report Rab11-FIP5 as a specific regulator of recycling of α6 integrin and is not involved in the recycling of the other laminin-binding α3 integrin that also dimerizes with the β1 integrin subunit. Moreover, according to previous reports, Rab11-FIP5 is not involved in trafficking of other integrins such as the fibronectin binding α5β1 integrin or the vitronectin receptor αvβ3, both being regulated by Rab11-FIP1 (11). Future experiments can determine if Rab11-Fip5 silencing would interfere with motility on ECM ligands other than laminin, including collagen, vitronectin and fibronectin. Additionally, we found Rab11-FIP5 did not affect membrane expression of other cell adhesion proteins, for example CD44, E-cadherin or of the transferrin receptor.

The membrane expression of both α6 and β4 integrins was dependent on Rab11-FIP5, raising an important question if it is an α6 or β4 dependent phenomenon. Since functional inhibition of Rab11-FIP5 had similar effects on α6 integrin membrane expression in β4 null

PC3 cell line, Rab11-FIP5 clearly can regulate α6 independent of β4. Earlier reports had shown the cytoplasmic tail sequence of α6 integrin was important for membrane expression of α6β4 integrin. Moreover, the cytoplasmic tail of α6 integrin was shown to be sufficient to signal trafficking of CD8, a receptor with no measurable internalization (38). We speculate the Rab11-FIP5 dependent regulation of α6β4 integrin is possibly directed by specific endocytic signal sequences present in the cytoplasmic tail of α6 integrin. The alpha subunits differ in their cytoplasmic tail sequences as well as their trafficking kinetics. We had earlier reported that the α6 and α3 integrins have different internalization kinetics (33). Here we found that their recycling rates and recycling locations are quite different as well. α6 integrin has a 2-fold higher recycling rate than α3 integrin and recycles in cell-cell locations as compared to the lamellipodia location for α3 integrin. This further emphasizes the role of alpha subunit in specifying intracellular trafficking routes of integrins. Future studies will be important to identify key motifs in the cytoplasmic tails of alpha subunits that provide the specificity of integrin trafficking.

Rab11-FIP5 regulated membrane expression of α6 integrin was functionally dependent on the C2 domain of Rab11-FIP5. The C2 domain is known to bind specific membrane phosphoinositides like phosphatidylinositol 3,4,5 trisphosphate (PIP3) and phosphatidic acid (24), and is crucial for docking of cargo containing Rab11 vesicles to the plasma membrane (24) before release of vesicular contents through exocytosis (39). Interestingly, we found that the recycled α6 integrin was mainly targeted to the lateral membrane locations of cell-cell adhesions. Determining if this was driven by the specific membrane phosphoinositide composition of the targeted areas will be an interesting avenue of future research.

In Rab11-FIP5 depleted cells, the internalization rate of α6 integrin was unaffected but the defect in recycling caused intracellular accumulation of α6 integrin. The resulting intracellularly accumulated integrins were found in both early endosomes and Rab11 endosomes, indicating that Rab11-FIP5 is not involved in trafficking of α6 from early endosomes to Rab11 but must be a regulator of trafficking of α6 integrin from Rab11 compartment to the plasma membrane.

Interestingly, we observed α6 integrin was recycled to cell-cell adhesions (Fig. 7). Additionally, there was a significant colocalization of α6 integrin with Rab11 at the cell-cell adhesion sites (Fig. 5). Depletion of Rab11-FIP5 significantly reduced such colocalization at the plasma membrane. Similar observations of α6 integrin recycling to the lateral cellular adhesions has been noted in model systems such as cultured human epidermal keratinocyte sheets (40) and developing basal epidermis of zebrafish (41). Moreover, Rab11 is important for cell-cell communication during collective migration in border cell cluster migration in *Drosophila* (42). The significance of targeting the recycled α6 integrin to the cell-cell adhesions of cancer cells is currently not understood. Integrins have been implicated in cell-cell adhesion (6, 43–45) by either direct interaction via intercellular ligand or indirectly by stabilization of E-cadherin mediated cell-cell adhesion complexes. The α6 integrin at lateral cell membrane locations can simply be a reservoir waiting to be recruited to cell-extracellular matrix adhesions (41). Alternatively, α6 integrin might be of functional importance for cell-cell adhesion as has been published previously (46).

Rab11-FIP5 was identified among top three genes of prognosis and poor outcome in ovarian cancer (47). Selective amplification of vesicular pathways involving specific integrins may be important in cancer progression. The results of the current study demonstrate that vesicular trafficking regulates the amount of α6 integrin at the cell surface of prostate cancer cells. In this cancer type, invasion and metastasis is significantly dependent on α6 integrin. α6 integrin is prominent in prostate cancer invasion, as well as in bone and visceral metastasis as a cohesive cluster phenotype (48, 49) which is targetable. We identified various intracellular trafficking regulatory proteins that are significantly associated with the ratio of intracellular to cell surface localization of α6 integrin. Excitingly, Rab11-FIP5 levels demonstrated the greatest association with cytoplasmic α6 integrin protein levels. Moreover, as prostate cancer cell migration on laminin-enriched surfaces were significantly dependent on Rab11-FIP5, we speculate that invasion into laminin-enriched nerves and metastases to laminin rich bone might be dependent on α6 integrin active recycling by Rab11-FIP5.

Supplementary Material

Refer to Web version on PubMed Central for supplementary material.

ACKNOWLEDGEMENTS

Rab11-FIP5-GFP mutant cDNA constructs were a kind gift from Dr. Rytis Prekeris. We thank Lucas Heppner who analyzed expression of β4 integrin in PC3N cells. We appreciate the support from Dr. Greg Rogers and his lab members for use of the Deltavision Core deconvolution microscope. We acknowledge the institutional support from Cedars Sinai Medical Center, Los Angeles, CA for immunohistochemistry analysis by their Biobank and Translational Research Core. We thank the patients and their families who were willing to participate in the Prostate Cancer Donor Program. Research at Cedars Sinai Medical Center was supported by Pacific Northwest Prostate Cancer SPORE (P50CA97186), the PO1 NIH grant (PO1CA085859) and the Richard M. LUCAS Foundation. Research at the University of Colorado was supported in part by NIH-NIDDK R01-DK064380 (R. Prekeris), research at the University of Arizona was supported in part by NIH-NCI RO1CA159406 (J.M.C. Gard, A.E. Cress), NIH-NCI RO1CA154835 (C. Miranti), P30CA23074 and The Tim and Diane Bowden Cancer Biology Fellowship Award (L. Das).

REFERENCES

1. Hood JD, Cheresh DA. Role of integrins in cell invasion and migration. Nature reviews Cancer. 2002;2:91–100. [PubMed: 12635172]
2. Georges-Labouesse E, Messaddeq N, Yehia G, Cadalbert L, Dierich A, Le Meur M. Absence of integrin alpha 6 leads to epidermolysis bullosa and neonatal death in mice. Nature genetics. 1996;13:370–3. [PubMed: 8673141]
3. Longmate WM, Dipersio CM. Integrin Regulation of Epidermal Functions in Wounds. Advances in wound care. 2014;3:229–46. [PubMed: 24669359]
4. Sonnenberg A, Calafat J, Janssen H, Daams H, van der Raaij-Helmer LM, Falcioni R, et al. Integrin alpha 6/beta 4 complex is located in hemidesmosomes, suggesting a major role in epidermal cell-basement membrane adhesion. The Journal of cell biology. 1991;113:907–17. [PubMed: 2026654]
5. Shimizu O, Shiratsuchi H, Ueda K, Oka S, Yonehara Y. Alteration of the actin cytoskeleton and localisation of the alpha6beta1 and alpha3 integrins during regeneration of the rat submandibular gland. Archives of oral biology. 2012;57:1127–32. [PubMed: 22410146]
6. Belvindrah R, Hankel S, Walker J, Patton BL, Muller U. Beta1 integrins control the formation of cell chains in the adult rostral migratory stream. The Journal of neuroscience : the official journal of the Society for Neuroscience. 2007;27:2704–17. [PubMed: 17344408]
7. Larjava H, Salo T, Haapasalmi K, Kramer RH, Heino J. Expression of integrins and basement membrane components by wound keratinocytes. The Journal of clinical investigation. 1993;92:1425–35. [PubMed: 8376596]

8. Underwood RA, Carter WG, Usui ML, Olerud JE. Ultrastructural localization of integrin subunits beta4 and alpha3 within the migrating epithelial tongue of in vivo human wounds. The journal of histochemistry and cytochemistry : official journal of the Histochemistry Society. 2009;57:123–42. [PubMed: 18824633]
9. Owens DM, Romero MR, Gardner C, Watt FM. Suprabasal alpha6beta4 integrin expression in epidermis results in enhanced tumourigenesis and disruption of TGFbeta signalling. Journal of cell science. 2003;116:3783–91. [PubMed: 12902406]
10. Bridgewater RE, Norman JC, Caswell PT. Integrin trafficking at a glance. Journal of cell science. 2012;125:3695–701. [PubMed: 23027580]
11. Caswell PT, Chan M, Lindsay AJ, McCaffrey MW, Boettiger D, Norman JC. Rab-coupling protein coordinates recycling of alpha5beta1 integrin and EGFR1 to promote cell migration in 3D microenvironments. The Journal of cell biology. 2008;183:143–55. [PubMed: 18838556]
12. Barr FA. Review series: Rab GTPases and membrane identity: causal or inconsequential? The Journal of cell biology. 2013;202:191–9. [PubMed: 23878272]
13. Stenmark H Rab GTPases as coordinators of vesicle traffic. Nature reviews Molecular cell biology. 2009;10:513–25. [PubMed: 19603039]
14. Goldenring JR. Recycling endosomes. Current opinion in cell biology. 2015;35:117–22. [PubMed: 26022676]
15. Caswell PT, Vadrevu S, Norman JC. Integrins: masters and slaves of endocytic transport. Nature reviews Molecular cell biology. 2009;10:843–53. [PubMed: 19904298]
16. Mosesson Y, Mills GB, Yarden Y. Derailed endocytosis: an emerging feature of cancer. Nature reviews Cancer. 2008;8:835–50. [PubMed: 18948996]
17. Yoon S-O, Shin S, Mercurio AM. Hypoxia Stimulates Carcinoma Invasion by Stabilizing Microtubules and Promoting the Rab11 Trafficking of the α6β4 Integrin. Cancer Research. 2005;65:2761–9. [PubMed: 15805276]
18. Strachan LR, Condic ML. Cranial neural crest recycle surface integrins in a substratum-dependent manner to promote rapid motility. The Journal of cell biology. 2004;167:545–54. [PubMed: 15520227]
19. Bretscher MS. Circulating integrins: alpha 5 beta 1, alpha 6 beta 4 and Mac-1, but not alpha 3 beta 1, alpha 4 beta 1 or LFA-1. The EMBO journal. 1992;11:405–10. [PubMed: 1531629]
20. Horgan CP, McCaffrey MW. The dynamic Rab11-FIPs. Biochemical Society transactions. 2009;37:1032–6. [PubMed: 19754446]
21. Baetz NW, Goldenring JR. Rab11-family interacting proteins define spatially and temporally distinct regions within the dynamic Rab11a-dependent recycling system. Molecular biology of the cell. 2013;24:643–58. [PubMed: 23283983]
22. Prekeris R, Davies JM, Scheller RH. Identification of a novel Rab11/25 binding domain present in Eferin and Rip proteins. The Journal of biological chemistry. 2001;276:38966–70. [PubMed: 11481332]
23. Meyers JM, Prekeris R. Formation of mutually exclusive Rab11 complexes with members of the family of Rab11-interacting proteins regulates Rab11 endocytic targeting and function. The Journal of biological chemistry. 2002;277:49003–10. [PubMed: 12376546]
24. Lindsay AJ, McCaffrey MW. The C2 domains of the class I Rab11 family of interacting proteins target recycling vesicles to the plasma membrane. Journal of cell science. 2004;117:4365–75. [PubMed: 15304524]
25. Schonteich E, Wilson GM, Burden J, Hopkins CR, Anderson K, Goldenring JR, et al. The Rip11/Rab11-FIP5 and kinesin II complex regulates endocytic protein recycling. Journal of cell science. 2008;121:3824–33. [PubMed: 18957512]
26. Cruz-Monserrate Z, O'Connor KL. Integrin α6β4 Promotes Migration, Invasion through Tiam1 Upregulation, and Subsequent Rac Activation. Neoplasia. 2008;10:408–IN1. [PubMed: 18472958]
27. Ports MO, Nagle RB, Pond GD, Cress AE. Extracellular engagement of alpha6 integrin inhibited urokinase-type plasminogen activator-mediated cleavage and delayed human prostate bone metastasis. Cancer Res. 2009;69:5007–14. [PubMed: 19491258]

28. Tran NL, Nagle RB, Cress AE, Heimark RL. N-Cadherin expression in human prostate carcinoma cell lines. An epithelial-mesenchymal transformation mediating adhesion withStromal cells. The American journal of pathology. 1999;155:787–98. [PubMed: 10487836]
29. Prekeris R, Klumperman J, Scheller RH. A Rab11/Rip11 protein complex regulates apical membrane trafficking via recycling endosomes. Molecular cell. 2000;6:1437–48. [PubMed: 11163216]
30. Roudier MP, True LD, Higano CS, Vesselle H, Ellis W, Lange P, et al. Phenotypic heterogeneity of end-stage prostate carcinoma metastatic to bone. Human pathology. 2003;34:646–53. [PubMed: 12874759]
31. Zhang X, Morrissey C, Sun S, Ketchandji M, Nelson PS, True LD, et al. Androgen receptor variants occur frequently in castration resistant prostate cancer metastases. PloS one. 2011;6:e27970. [PubMed: 22114732]
32. Nguyen HM, Vessella RL, Morrissey C, Brown LG, Coleman IM, Higano CS, et al. LuCaP Prostate Cancer Patient-Derived Xenografts Reflect the Molecular Heterogeneity of Advanced Disease and Serve as Models for Evaluating Cancer Therapeutics. The Prostate. 2017;77:654–71. [PubMed: 28156002]
33. Das L, Anderson TA, Gard JM, Sroka IC, Strautman SR, Nagle RB, et al. Characterization of Laminin Binding Integrin Internalization in Prostate Cancer Cells. Journal of cellular biochemistry. 2017;118:1038–49. [PubMed: 27509031]
34. Wiley HS, Cunningham DD. The endocytotic rate constant. A cellular parameter for quantitating receptor-mediated endocytosis. The Journal of biological chemistry. 1982;257:4222–9. [PubMed: 6279628]
35. Junutula JR, Schonteich E, Wilson GM, Peden AA, Scheller RH, Prekeris R. Molecular characterization of Rab11 interactions with members of the family of Rab11-interacting proteins. The Journal of biological chemistry. 2004;279:33430–7. [PubMed: 15173169]
36. Willenborg C, Jing J, Wu C, Matern H, Schaack J, Burden J, et al. Interaction between FIP5 and SNX18 regulates epithelial lumen formation. The Journal of cell biology. 2011;195:71–86. [PubMed: 21969467]
37. Ullrich O, Reinsch S, Urbe S, Zerial M, Parton RG. Rab11 regulates recycling through the pericentriolar recycling endosome. The Journal of cell biology. 1996;135:913–24. [PubMed: 8922376]
38. Gaietta G, Redelmeier TE, Jackson MR, Tamura RN, Quaranta V. Quantitative measurement of alpha 6 beta 1 and alpha 6 beta 4 integrin internalization under cross-linking conditions: a possible role for alpha 6 cytoplasmic domains. Journal of cell science. 1994;107 (Pt 12):3339–49. [PubMed: 7706390]
39. Takahashi S, Kubo K, Waguri S, Yabashi A, Shin HW, Katoh Y, et al. Rab11 regulates exocytosis of recycling vesicles at the plasma membrane. Journal of cell science. 2012;125:4049–57. [PubMed: 22685325]
40. Poumay Y, Leclercq-Smekens M, Grailly S, Degen A, Leloup R. Specific internalization of basal membrane domains containing the integrin alpha 6 beta 4 in dispase-detached cultured human keratinocytes. European journal of cell biology. 1993;60:12–20. [PubMed: 8462591]
41. Sonawane M, Martin-Maischein H, Schwarz H, Nusslein-Volhard C. Lgl2 and E-cadherin act antagonistically to regulate hemidesmosome formation during epidermal development in zebrafish. Development. 2009;136:1231–40. [PubMed: 19261700]
42. Ramel D, Wang X, Laflamme C, Montell DJ, Emery G. Rab11 regulates cell-cell communication during collective cell movements. Nature cell biology. 2013;15:317–24. [PubMed: 23376974]
43. Larjava H, Peltonen J, Akiyama SK, Yamada SS, Gralnick HR, Uitto J, et al. Novel function for beta 1 integrins in keratinocyte cell-cell interactions. The Journal of cell biology. 1990;110:803–15. [PubMed: 1689734]
44. Kaufmann R, Frosch D, Westphal C, Weber L, Klein CE. Integrin VLA-3: ultrastructural localization at cell-cell contact sites of human cell cultures. The Journal of cell biology. 1989;109:1807–15. [PubMed: 2677029]

45. Hegerfeldt Y, Tusch M, Bröcker E-B, Friedl P. Collective Cell Movement in Primary Melanoma Explants: Plasticity of Cell-Cell Interaction, β1-Integrin Function, and Migration Strategies. Cancer Research. 2002;62:2125–30. [PubMed: 11929834]

46. Emsley J α6β1 integrin directs migration of neuronal precursors in adult mouse forebrain. Experimental Neurology. 2003;183:273–85. [PubMed: 14552869]

47. Willis S, Villalobos VM, Gevaert O, Abramovitz M, Williams C, Sikic BI, et al. Single Gene Prognostic Biomarkers in Ovarian Cancer: A Meta-Analysis. PloS one. 2016;11:e0149183. [PubMed: 26886260]

48. Harryman WL, Hinton JP, Rubenstein CP, Singh P, Nagle RB, Parker SJ, et al. The Cohesive Metastasis Phenotype in Human Prostate Cancer. Biochimica et biophysica acta. 2016;1866:221–31. [PubMed: 27678419]

49. Harryman WL, Gard JMC, Pond KW, Simpson SJ, Heppner LH, Hernandez-Cortes D, et al. Targeting the Cohesive Cluster Phenotype in Chordoma via beta1 Integrin Increases Ionizing Radiation Efficacy. Neoplasia. 2017;19:919–27. [PubMed: 28954241]

IMPLICATIONS:

Rab11-FIP5 dependent α6β1 integrin recycling may be selectively targeted to limit migration of prostate cancer cells into laminin-rich tissues.

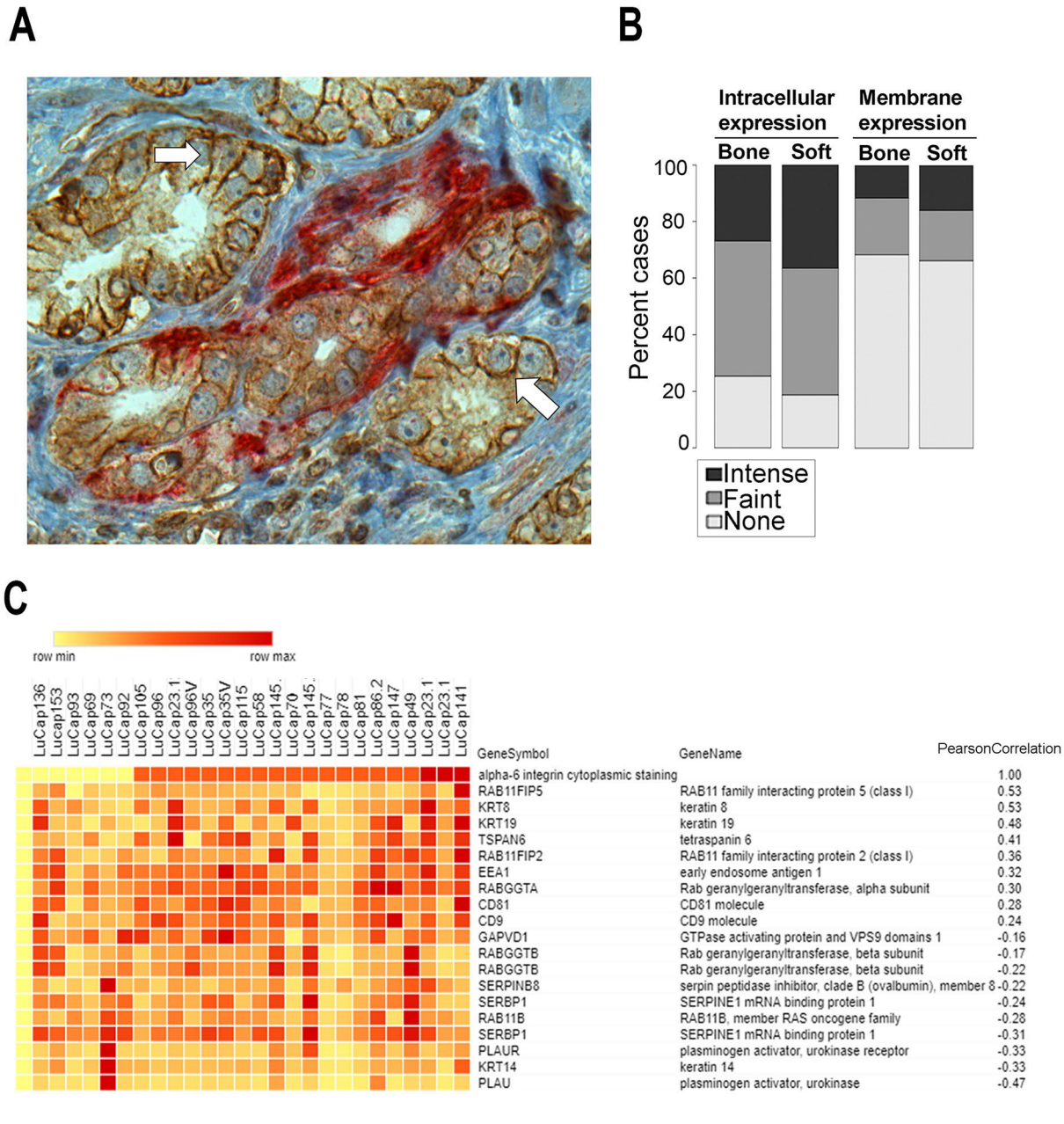

Figure 1. Intracellular expression of α6 integrin in aggressive human prostate cancer correlated with Rab11-FIP5 mRNA expression.

(A) Human prostate cancer reacted with antibody specific for α6 integrin (AA6NT, brown) or antibody specific for PGP 9.5, a neural specific marker (red). Membrane staining of α6 integrin (solid white arrows) is distinct from the cytoplasmic α6 integrin staining within aggressive cancer that is invading nerve (red). Scale Bar, 100μm. **(B)** Established LuCaP patient-derived xenografts (PDXs) and one hundred and eighty-five castration-resistant prostate cancer metastases (121 bone metastases and 64 soft tissue metastases) were investigated for localization of α6 integrin by immunostaining with AA6NT. Intracellular versus the membrane staining intensity were scored for absence or presence of faint or intense staining of α6 integrin. **(C)** Genome wide gene expression analysis and α6 integrin

immunohistochemical analysis of subcutaneous LuCaP PDX tissues were evaluated to identify genes correlated with cytoplasmic expression of integrin α6. Top 20 intracellular trafficking regulators with either significant positive or negative Pearson coefficient of correlation to cytoplasmic α6 integrin are reported. Rab11FIP5 was identified as the top candidate.

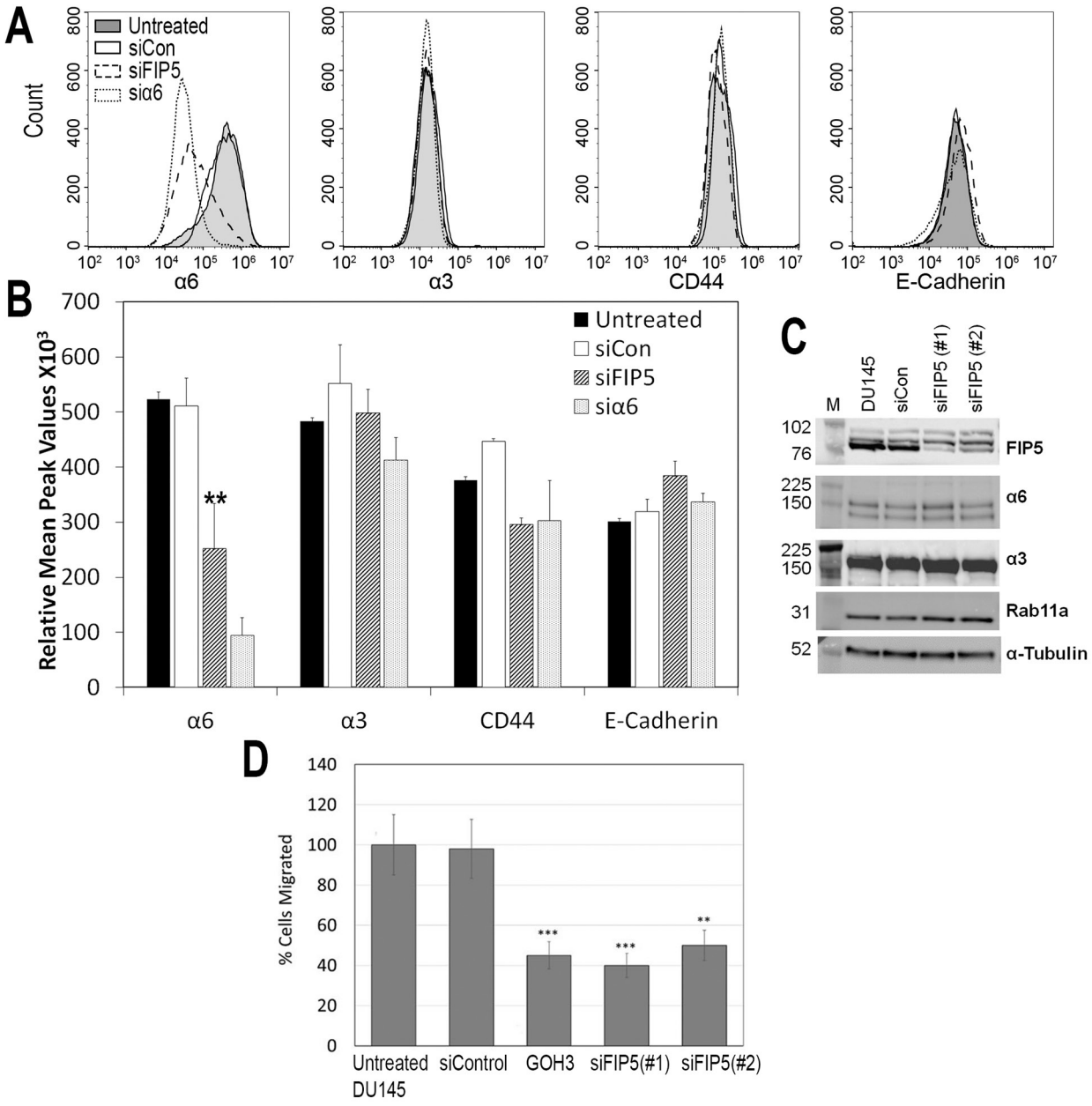

Figure 2. Rab11-FIP5 regulates membrane expression of α6 integrin and cancer cell migration.

DU145 cells were either untreated or transfected with non-targeting siRNA (siCon), siRNA against Rab11-FIP5 (siFIP5) or siRNA against α6 integrin (si α6). **(A)** Flow histograms of cell surface expression of laminin binding integrin subunits α6 or α3 and unrelated adhesion receptors CD44 and E-cadherin using immunolabelling of receptors in fixed, non-permeabilized untreated (solid line, shaded), siCon (solid line), siFIP5 (dashed line) and si α6 (dotted line) cells. **(B)** Relative mean peak fluorescence values of cell membrane expression of the receptors in untreated, siCon, siFIP5 and si α6 cells (**p<0.01, n=5). **(C)** Total cell lysate of untreated (DU145), siCon (siCon) and cells treated with two different siRNA against Rab11-FIP5 (siFIP5 #1, #2) immunoblotted for Rab11-FIP5 (FIP5), α6, α3, Rab11a and α-tubulin. **(D)** Untreated and DU145 cells treated with non-targeting siRNA

(siControl), α6 integrin function blocking antibody (GOH3), siRNA against Rab11-FIP5 (siFIP5#1) and (siFIP5#2) and were allowed to migrate in a modified Boyden chamber with 8μm pores in response to laminin enriched HaCaT conditioned media for 6 hours. Percent untreated or treated cells migrated were counted in 50 fields of view per sample (n=3, each experiment in triplicates). Statistical significance assessed by student's unpaired t-test (**p<0.01, ***p<0.001).

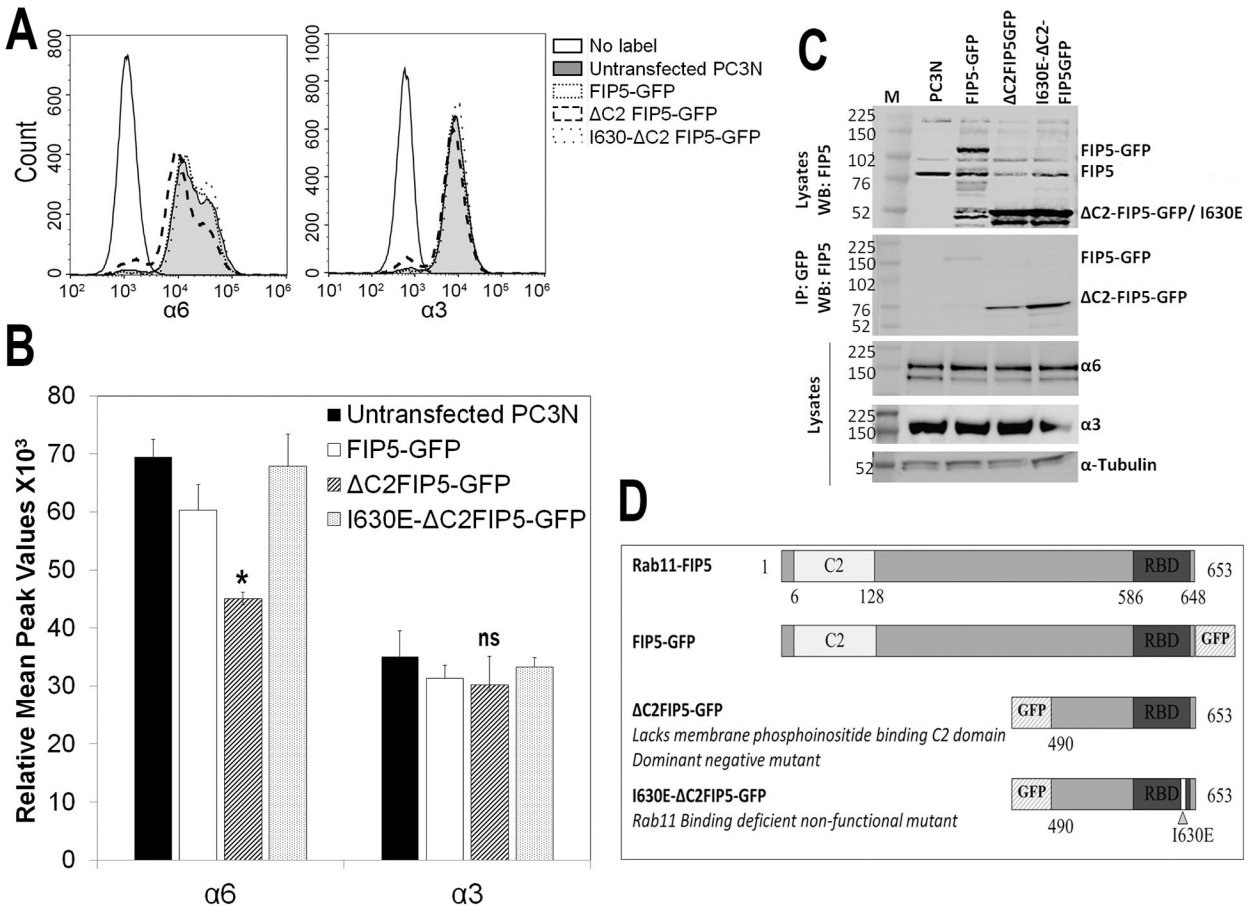

Figure 3. C2 domain of Rab11-FIP5 is required for the membrane expression of α6β1 integrin.

Rab11-FIP5 mutants tagged with GFP were stably transfected into PC3N cell line. The three different mutant containing cells are: (i) GFP tagged full length Rab11-FIP5 (ii) GFP tagged truncated Rab11-FIP5 protein lacking C2 domain (ΔC2FIP5-GFP) or (iii) a non-functional, Rab11 binding deficient, truncated Rab11-FIP5 mutant tagged with GFP (I630E-ΔC2FIP5-GFP) used as a vector control. **(A)** Flow histograms of cell surface expression of α6 and α3 subunits in untransfected and mutant FIP5-GFP transfected cells. **(B)** Relative mean peak fluorescence values of cell membrane expression of the integrin subunits in untreated and FIP5-GFP mutant transfected cells (ANOVA, *p<0.05, ns, not significant, n=4). **(C)** Total cell lysate of mutant FIP5-GFP transfected stable cell lines immunoblotted for Rab11-FIP5 protein show expression of endogenous (FIP5) and overexpressed GFP tagged full length or truncated FIP5 proteins. Immunoprecipitation of GFP protein shows expression of GFP-tagged mutant Rab11-FIP5 proteins. Total expression of α6 and α3 integrin subunits is shown. **(D)** Schematic representation of the FIP5-GFP mutants used.

A

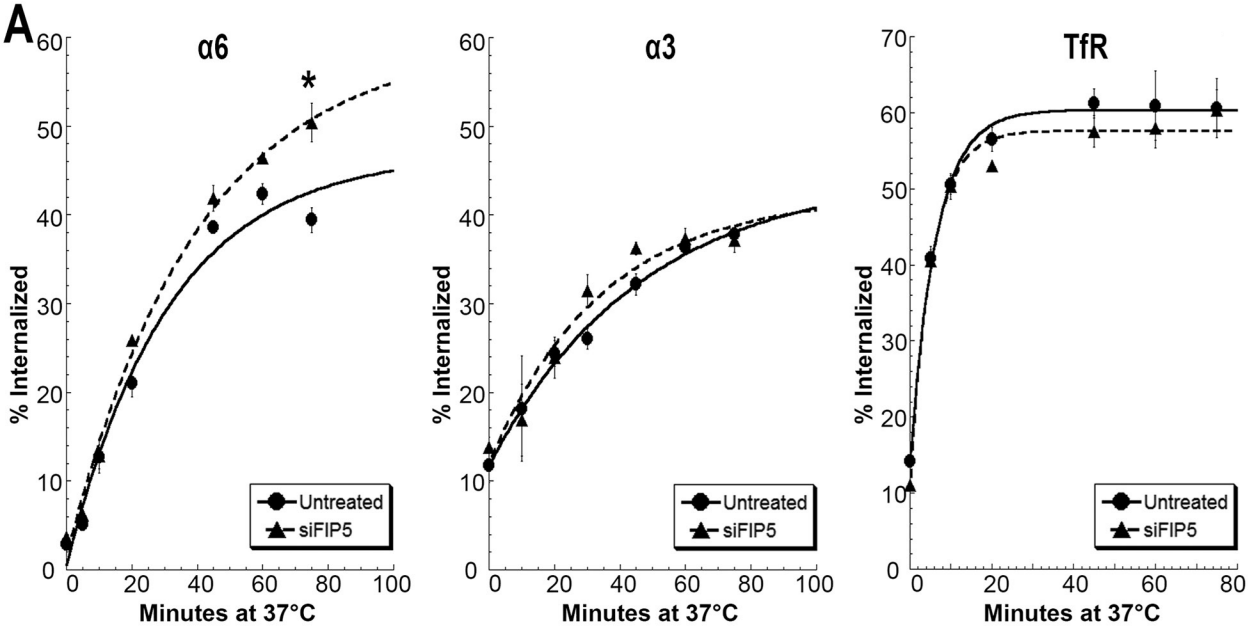

B

	α6 Internalization			α3 Internalization			TfR Internalization		
	Intracellular accumulation (%)	k_{obs} (min^{-1})	k_{actual} (min^{-1})	Intracellular accumulation (%)	k_{obs} (min^{-1})	k_{actual} (min^{-1})	Intracellular accumulation (%)	k_{obs} (min^{-1})	k_{actual} (min^{-1})
Untreated	46.33±4.85	0.032±0.009	1.48±0.57	32.91±3.04	0.021±0.004	0.69±0.19	57.62±2.5	0.18±0.024	10.37±1.83
siFIP5	58.16±4.83*	0.025±0.005	1.45±0.41	30.17±4.46	0.029±0.011	0.87±0.46	60.38±1.42	0.16±0.011	9.66±0.89

Figure 4. Depletion of Rab11-FIP5 expression increases intracellular accumulation of α6 integrin.

(A) Internalization kinetic curve for α6 integrin, α3 integrin or TfR in untreated DU145 and siFIP5 cells. Percent surface labeled receptors internalized is plotted for different time points at 37°C and fitted with a first order kinetic curve (R^2>0.989). **(B)** Maximum intracellular accumulation and internalization rate constants (observed, k_{obs} and actual, k_{actual}) calculated as per first order rate kinetics. Results represent 5 independent experiments. Statistical significance calculated for changes in label internalized at each timepoint and intracellular accumulation as per student's t-test, unpaired, *p<0.05, n=5.

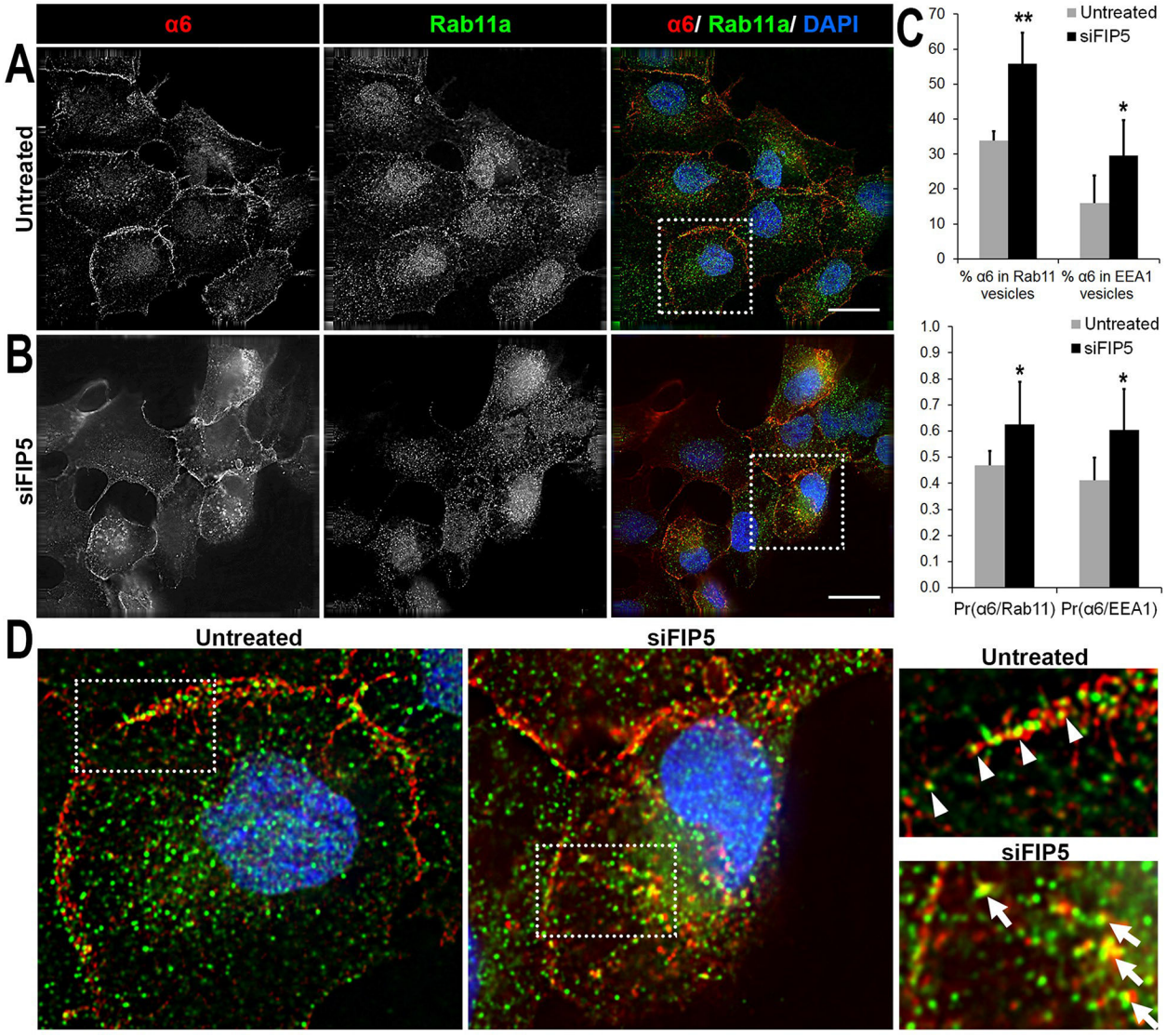

Figure 5. Distribution of α6 integrin in Rab11a vesicles.

Surface α6 integrin was labelled with J1B5 rat monoclonal antibody in DU145 cells and allowed to internalize for 40 minutes at 37°C. Cells were fixed, permeabilized, and immunostained for markers of intracellular vesicular compartments (EEA1 or Rab11a). Cellular distribution of α6 integrin and Rab11a vesicles in **(A)** Untreated DU145 cells and **(B)** siFIP5 treated cells. α6 integrin (red), Rab11a positive recycling vesicles (green) and DAPI (blue) in merged images. Images acquired by deconvolution microscopy and single Z-plane is shown. Bars, 20μm. (Image sections for cells co-stained for α6 integrin and EEA1 are provided in Supplementary Figure 1). **(C)** Percent α6 integrin in Rab11a and EEA1 vesicles is reported for untreated or siFIP5 cells based on 10 different fields of view in 4 independent experiments. Mean Pearson coefficients of correlation of α6 integrin with Rab11a (Pr(α6/Rab11)) or with EEA1 (Pr(α6/EEA1)) are also shown (*p<0.05 **p<0.01, n=4). **(D)** Magnified images of boxed sections for untreated and siFIP5 DU145 cells. Areas of interest are further magnified and marked for colocalization. The α6 integrin and Rab11a

colocalize at cell-cell membrane locations (white triangles), mainly observed in untreated cells. Intracellular colocalization of α6 integrin and Rab11a (white arrows) is prominent in siFIP5 cells.

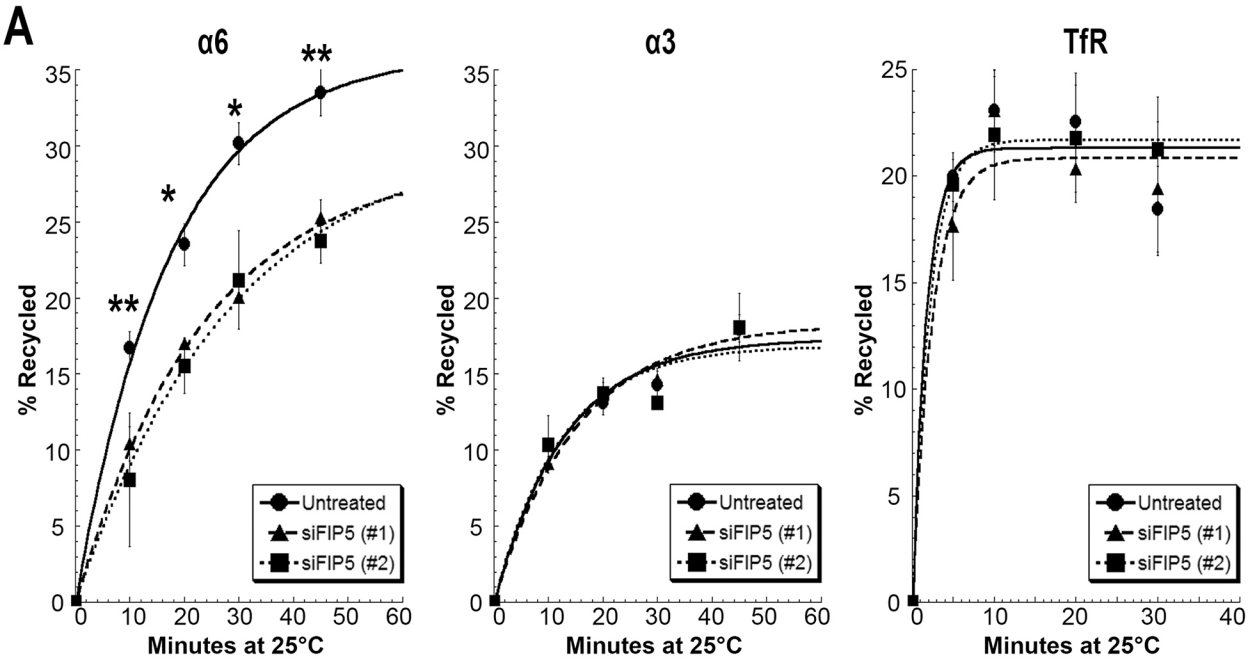

B

	α6 Recycling			α3 Recycling			TfR Recycling		
	Maximum label recycled (%)	k_{obs} (min^{-1})	k_{actual} (min^{-1})	Maximum label recycled (%)	k_{obs} (min^{-1})	k_{actual} (min^{-1})	Maximum label recycled (%)	k_{obs} (min^{-1})	k_{actual} (min^{-1})
Untreated	36.14±1.82	0.057±0.007	2.06±0.35	17.33±1.75	0.077±0.023	1.33±0.53	21.72±0.69	0.512±0.16	11.12±3.82
siFIP5 (#1)	29.15±2.11 *	0.042±0.006	1.22±0.26**	18.32±1.35	0.066±0.013	1.21±0.32	20.86±1.23	0.489±0.16	10.20±3.93
siFIP5 (#2)	30.73±4.26 *	0.035±0.008	1.08±0.39**	16.87±2.32	0.082±0.035	1.38±0.78	21.7±0.27	0.474±0.05	10.29±1.21

Figure 6. Depletion of Rab11-FIP5 expression reduces recycling of α6 integrin.

DU145 cells were transfected with two different siRNAs against Rab11-FIP5: siFIP5(#1) or siFIP5(#2) **(A)** Recycling kinetic curve for α6 integrin, α3 integrin or TfR in untreated and siFIP5 DU145 cells. Percent label recycled to the cell surface at 25°C (calculated as percent mean peak fluorescence of recycled label at a given timepoint vs total label internalized) is plotted for different time intervals. First order kinetic curve is fitted (R^2>0.98). **(B)** Maximum label recycled (%) and recycling rate constants (observed, k_{obs} and actual, k_{actual}) calculated as per first order rate kinetics. Results represent 5 independent experiments. Statistical significance calculated for changes in label recycled at each timepoint and maximum label recycled as per student's t-test, unpaired, *p<0.05 **p<0.01, n=5.

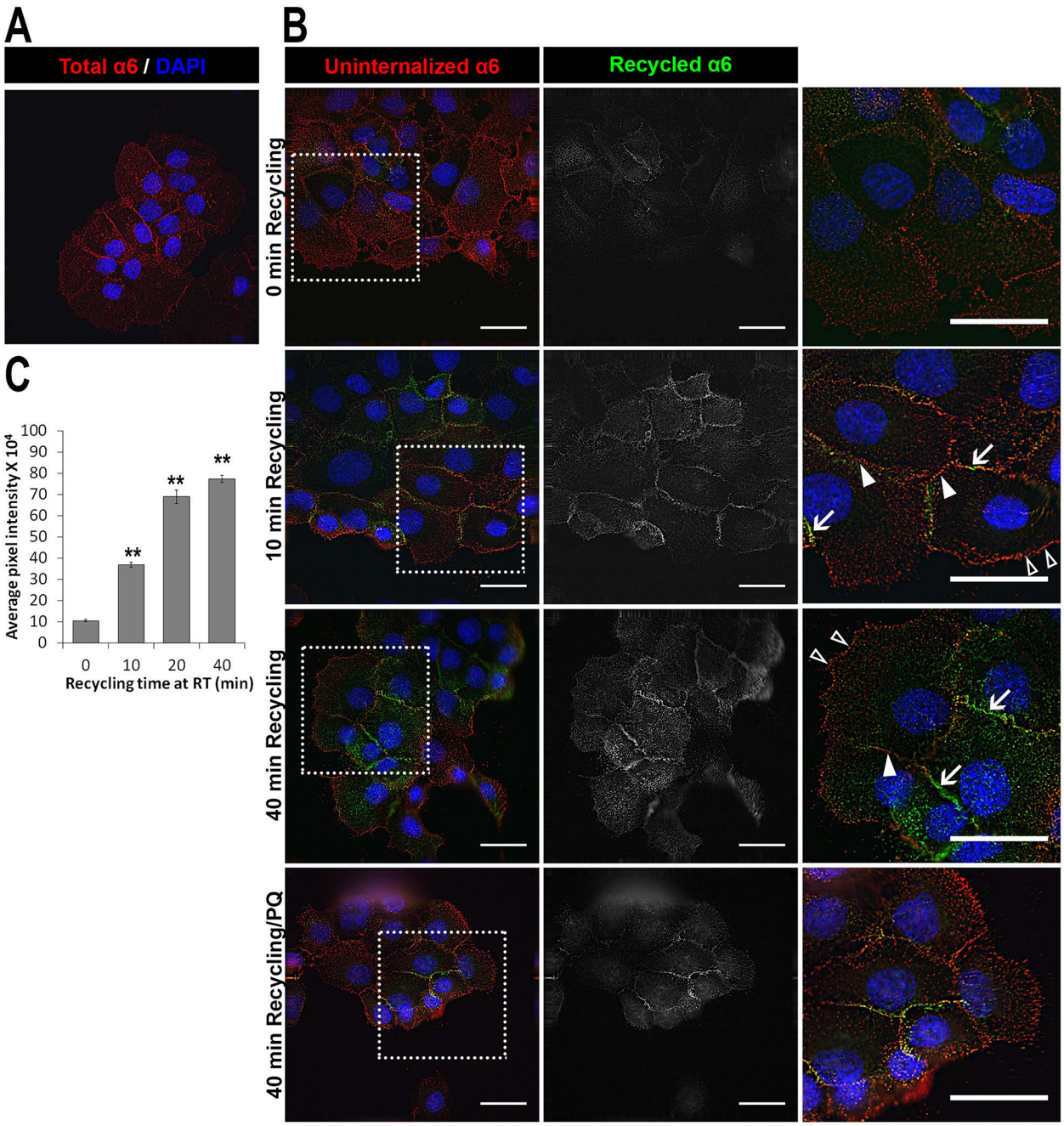

Figure 7. α6 integrin recycled to cell-cell lateral membrane locations.

Surface α6 integrin was labelled with J1B5 rat monoclonal antibody in DU145 cell monolayer and allowed to internalize for 40 minutes at 37°C. Uninternalized label at the cell membrane is blocked using Alexa 568 conjugated anti-rat secondary antibody. J1B5 antibody bound integrin protected inside the cells was allowed to recycle back and subsequently reacted with Alexa 488 conjugated anti-rat secondary antibody. **(A)** Total membrane and internalized intracellular α6 integrin in permeabilized cells shown as control (red). **(B)** Uninternalized α6 integrin (red) and recycled α6 integrin (green) at 0 min, 10 min and 40 minutes of recycling and 40 min recycling with primaquine (PQ, recycling inhibitor)

are shown in merged images with DAPI (blue) stained nucleus (left panel). Middle panel shows only recycled α6 integrin label in gray. Right panel is magnified images of boxed sections marked for recycled integrin localized at cell-cell membrane locations (white arrows), uninternalized integrin at cell-cell locations (closed white triangles) and lamellipodia at cell front (open white triangles). Images acquired by deconvolution microscopy and single Z-plane is shown. Bars, 20μm **(C)** Bar graph showing average pixel intensity of recycled label plotted for different timepoints of recycling at room temperature (RT) (**p<0.01, 10 field of views in 3 independent experiments).